

Research on Motion Stability of High-Speed Trains under Cross-Wind Effect

Yuming Yang, Xiangning Wang, Yingzheng Zhao, Jun Mao and Yanhong Xi

School of Civil Engineering and Architecture, Beijing Jiaotong University, Beijing 100044, China

*Corresponding author

Abstract—By taking real domestic CRH high-speed trains as research object, using the Computational Fluid Dynamics software Starccm+ to carry out numerical simulation calculations when the train runs in different vehicle speeds and cross-wind speeds, We get aerodynamic loads in diverse working conditions. Furthermore, these loads are introduced into the Dynamics Simulation Software SIMPACK, which calculates some running stability parameters such as the derailment coefficient and the reduction rate of wheel load in different cross-wind and vehicle speeds. The calculation indicates that the higher the wind speed is, the lower the vehicle's maximum operating speed is and vice versa.; the maximum safe operating speed varies with different safety index limits, which can offer reference for the control of the train's running safety under cross winds. (*Abstract*)

Keywords—high-speed trains; aerodynamic loads; wheel-rail dynamics; motion stability; simulation calculation

I. INTRODUCTION

High-speed trains possess very complex three-dimensional geometric shape and big slenderness ratio, therefore the high-speed running forms a complex and strongly nonlinear 3-D viscous flow. When the train runs in cross-wind condition, its circle flow field and aerodynamic characteristics will change acutely, the performance of Wheel-Rail Dynamics will vary as well. As a consequence, the train's motion stability will be affected. About the research on cross-wind effect and aerodynamic safety, many achievements have been obtained so far at home and abroad. But it's necessary to research deeper into such fields as modeling complicated scenes, analysis of cross-wind aerodynamic forces and the influence of cross-wind aerodynamic characteristics on the train's running safety. This article analyses the aerodynamic characteristics of high-speed trains under cross winds, and figures out aerodynamic loads acting on the train. In addition, using Vehicle-track Dynamics theory and Multi-body Dynamics simulation, We apply the cross-wind aerodynamic loads to the train in motion, get kinetic parameters under the cross winds, and the influence of cross wind on motion stability.

II. AERODYNAMICS CALCULATION OF HIGH-SPEED TRAINS WORKING IN CROSSWIND

To precisely calculate the three-dimensional aerodynamic force of CRH3 when moving at high speed in crosswind, the geometric model adopted is as similar to the real train as possible. In the numerical simulation, the model is complex

with numerous grids, so the fluid mechanics software Star-CD/CCM+ is used for parallel computing.

A. The Calculation Model and Conditions

The middle section fo the train remains unchanged, and basic characteristics of the flow field structure of the train are not changed by the abbreviated model [4]. 3 trains are combined as one group, that is, the head train + trailing train + tail train. There lengths are 25.675 m , 24.775 m , and 25.675 m respectively. The train is 3.265m wide and 3.89m high. Detailed structure like the bogie, pantograph and windshield are taken into account in the model.

Mainly computed working conditions are:

(1) The train speed is 200, 250, 300, 350, and 380km/h; The boundary speed of the lower atmosphere is adopted as the crosswind. According to literature [5], the wind speed at the height of 10m is 10, 15, 20, 25, and 30m/s meteorologically, and the crosswind direction is 90°.

(2) $k-\omega$ turbulence model and finite volume method are used. The diffusion term is discreted by the second-order precise central difference scheme, while the second-order upwind scheme discretizing is applied to the convective term. The separated type of solution is utilized for calculation of discrete governing equations.

B. The Computational Domain and Meshing

The computational domain and meshing are shown in Fig.1 and Fig.2. The hexahedral mesh is used to form a boundary layer on the train surface and the ground. Grids of areas with significant fluctuation of the flow field such as the wake stream, train surface and pantograph are denser. The total number of grids in the whole computation zone is approximately 31 million.

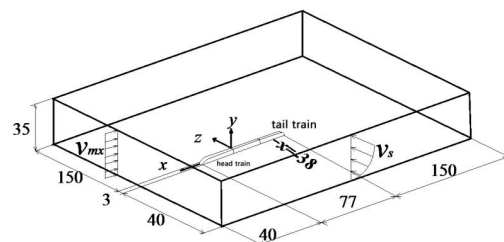


FIGURE 1. THE COMPUTATIONAL DOMAIN OF EXTERNAL FLOW FIELD SIMULATION OF THE CRH HIGH-SPEED TRAIN(UNIT: M)

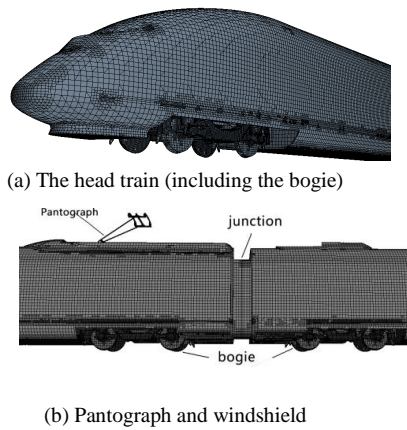


FIGURE II. LOCAL MESHING DOMAIN OF THE TRAIN

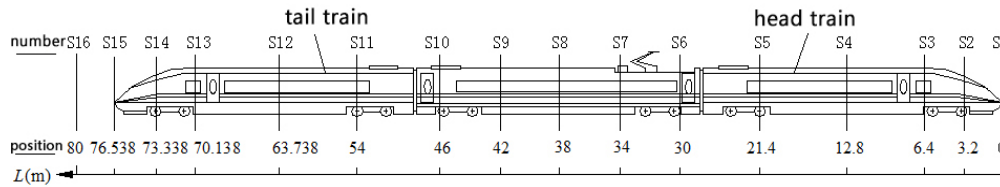


FIGURE III. THE LONGITUDINAL CROSS-SECTION POSITION OF THE TRAIN

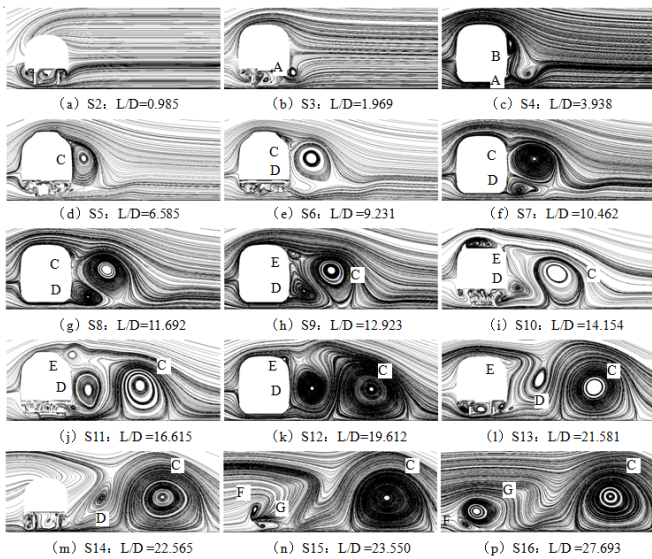


FIGURE IV. THE CROSS-SECTION FLOW PATTERN OF THE TRAIN (THE CROSSWIND DIRECTION IS FROM LEFT TO RIGHT)

At $L/D=3.938$, the second separation vortex B has been generated (in the different direction of turning from the vortex A); Then, in the range from $L/D=3.938$ to $L/D=6.585$, A and B gradually mix together to form a new separation vortex C which begins from the end of the head train $L/D=6.585$ and remains till the wake stream of the train $L/D=27.693$. However, its geometric dimension and distance away from the leeward side are gradually increased, and the former reaches the maximum at the initial section of the streamline body of the tail train $L/D=21.581$.

The initial separation vertex D is triggered when the separation vertex C is away from the leeward side $L/D=9.231$.

C. Flow Field Structure

The flow field structure of different sections is analyzed when the train speed is 300km/h and the crosswind speed is 30m/s. Fig.3 shows the longitudinal cross-section position of the train, and Fig.4 shows the flow pattern of different sections in the longitudinal or x-axis direction of the train, where L is the train length and D is the train width.

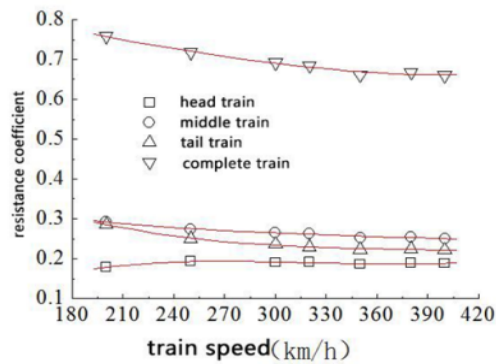
As can be learnt from Fig.4, at the longitudinal distance $L/D=1.969$, that is, the section position of the streamline body end of the head train, only one separation vortex A with insignificant fluctuation is generated below the leeward side.

The separation vertex D is formed completely at $L/D=10.462$, and it remains till the tail section of the train $L/D=22.565$ before basically maintaining in the lower position of the leeward side. Its geometric dimension witnesses a rise before the subsequent drop, which is in the unsteady status. In addition, at the section affected by the pantograph or air inlet and outlet of the air conditioning, an additional separation vortex E is generated on the top right corner of the leeward side. As the asymmetric separation vortex F and G are produced at the nose cone due to the removal of airflow from the train surface, the two vertexes are expanded gradually in the wake flow below the nose cone of the tail train (e.g. $L/D=27.693$) before being crushed into smaller turbulent vortexes far away. In the process, clear small-scale separation vortexes can be seen on the pantograph base at S10 section $L/D=14.154$

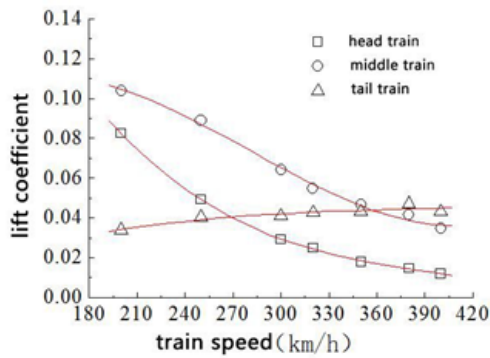
D. Aerodynamic Load of the High-Speed Train Working in Crosswind

Fig.5 shows the curve of relationship between aerodynamic forces and applied moment coefficients and the train speed. The crosswind speed in various working conditions is always 15m/s. As can be seen from Fig.5, the resistance coefficient is slightly and steadily decreased with the increase of the train speed, and it tends to be stable when the train speed is constant. The lift coefficient of the middle train is always larger than that of the head train, and it decreases as the train speed becomes higher. The lift of the tail train is smaller than that of the head train and middle train when the train speed is low. However, as the speed becomes higher, it surges rapidly. When the train speed is 350km/h, it even surpasses the lift of the head train and the middle train, which is mainly a result of the reduced surface pressure of the streamline body of the tail train caused by the increasing train speed and strengthening separation flow. The overturning moment coefficient of the head train crossing the longitudinal axis of the train center is the maximum, followed

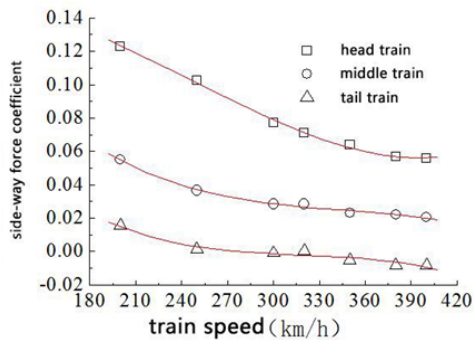
by that of the middle train, while that of the tail train is the minimum. Regarding to side-way moment, the head train is the maximum, followed by the tail train, while the middle train is the minimum. As for the pitching moment, the head train is the maximum.



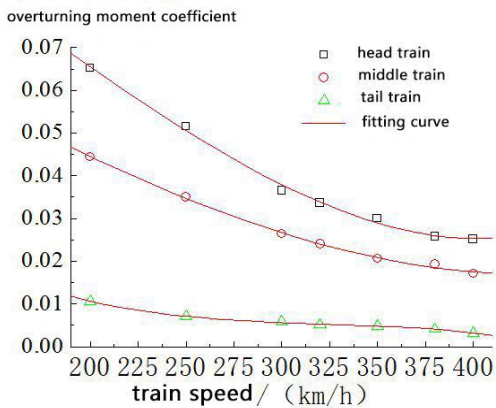
(a) resistance coefficient



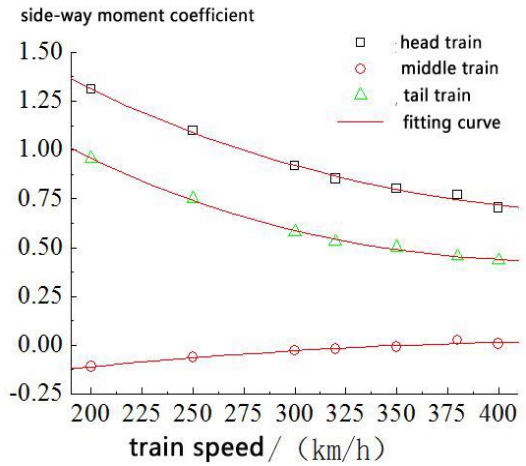
(b) lift coefficient



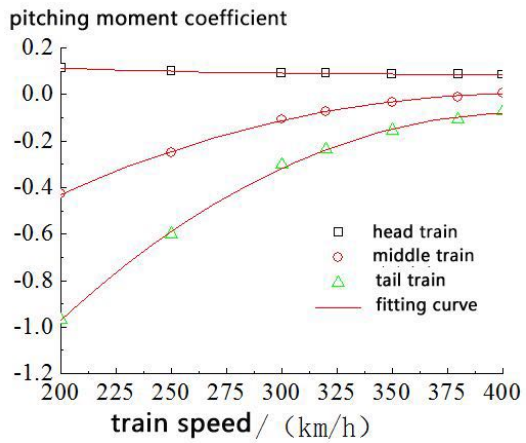
(c) side-way force coefficient



(d) Overturning moment coefficient



(e) Side-way moment coefficient



(f) Pitching moment coefficient

FIGURE V. RELATIONSHIP BETWEEN AERODYNAMIC FORCES AND MOMENT COEFFICIENTS AND THE TRAIN SPEED

III. DYNAMIC SIMULATION OF HIGH-SPEED TRAIN UNDER THE EFFECT OF CROSS WINDS

A. The Model of Dynamic SIMULATION

Correspond with the aerodynamic model, A high-speed train dynamics model consist of head car, trail car and tail car is established, as shown in FIG. 7. Each vehicle model in multiple unit is consist of vehicle body, bogie frame and wheelset. Each bogie comprises axle box suspension and central suspension. Axle box suspension includes vertical spring rate, lateral spring rate, longitudinal spring rate and damping of vertical damper. Central suspension is air springs, which include vertical, lateral, longitudinal nonlinear spring rate and damping of damper. There are six degrees of freedom in body and bogie and there are vertical, lateral, yaw and roll freedom in wheelset. Three carriages are sequentially connected in that order by the coupler raft gears. The model also includes some nonlinear parts which are more complete wheel-rail contact geometric relationship, lateral snubber, anti-hunting motion dampers and so on.

Using actual S1002G wheel tread to match the rail of 60 kg/m; Consider the nonlinearity of wheel-rail creep and the nonlinear characteristics of primary lateral and vertical damper, secondary lateral and vertical damper as well as lateral stop in

vehicle system; Based on equivalent Hertzian contact characteristics, using Fastsim algorithm of rolling contact nonlinear theory which is simplified by Kalker to calculate

creep force and creep moment between wheel and rail. Using German track spectrum to be the input about stochastic excitation of track.

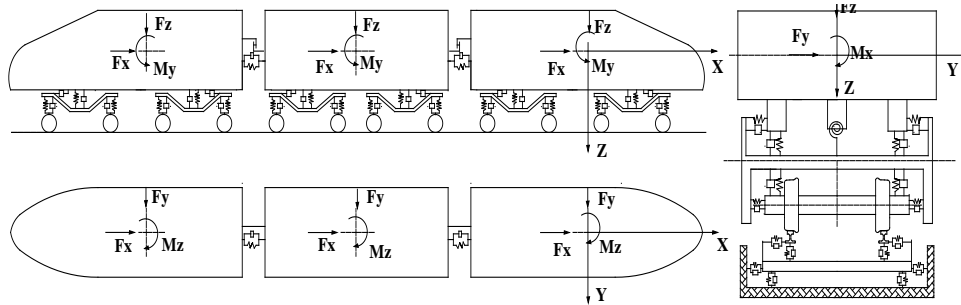


FIGURE VI. THE HIGH-SPEED TRAIN DYNAMICS MODEL UNDER THE EFFECT OF CROSS WIND

B. The Result of Dynamic Simulation

The calculation conditions of dynamic Simulation correspond to the aerodynamic load and we get the parameters

of operation dynamic in different train speed and different cross winds speed.

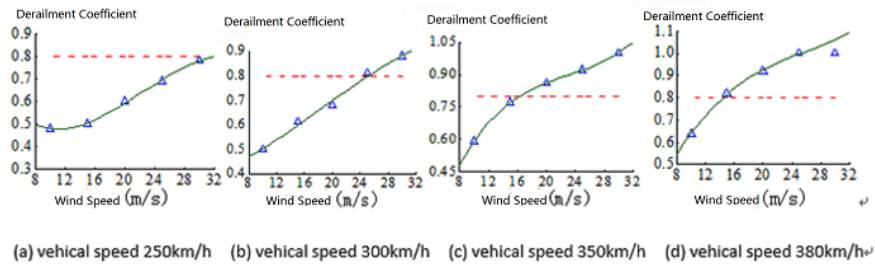


FIGURE VII. THE FUNCTIONAL CURVE BETWEEN THE SPEED OF CROSSWIND AND THE MAXIMAL VALUE OF DERAILMENT COEFFICIENT

FIG 7 illustrates the functional curve between the speed of crosswind and the maximal value of derailment coefficient. According to the figure, if the vehicle speed is 250km/h, the derailment coefficient is over the limit when the speed of cross wind is beyond 30 km/h; If the vehicle speed is 300 km/h, the derailment coefficient is over the limit when the speed of cross

wind is beyond 25 km/h; If the vehicle speed is 350 km/h, the derailment coefficient is over the limit when the speed of cross wind is beyond 30 km/h; If the vehicle speed is 380 km/h, the derailment coefficient is over the limit when the speed of cross wind is beyond 15 km/h.

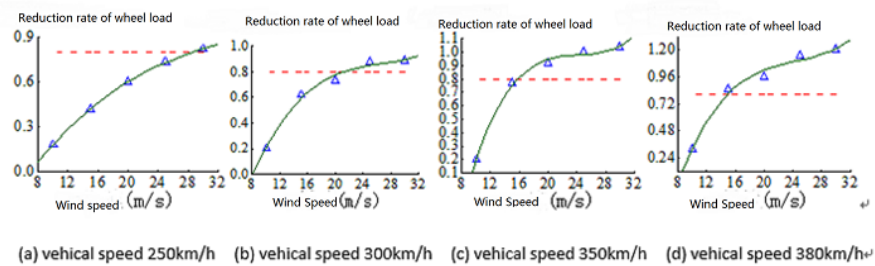


FIGURE VIII. THE FUNCTIONAL CURVE BETWEEN THE SPEED OF CROSSWIND AND THE MAXIMUM REDUCTION RATE OF WHEEL LOAD

Figure 8 illustrates the functional curve between the speed of cross winds and the maximum reduction rate of wheel load. According to the figure, all the maximum reduction rate of wheel load of the heading compartment show the same changing when the vehicle speed change and the tendency of its speed alteration increase as the vehicle speed increases. When the vehicle speed is 350km/h, the maximum reduction rate of wheel load of this vehicle is within safety limit.

However, when the vehicle runs with a speed of 300km/h, its maximum reduction rate of wheel load is beyond the safety value under a wind speed of 25m/s. Likewise, the maximum reduction rate of wheel load exceeds its safety limit when the vehicle speed are 350km/h and 380km/h under the wind speed of 20m/s and 15m/s respectively.

Based on these analyses, what we can conclude is that the higher the wind speed is, the lower the vehicle's maximum

operating speed is and vice versa.; the maximum safe operating speed varies with different safety index limits. We suggest taking both derailment coefficient and the reduction rate of wheel load as the basis for determining the maximum safe operating speed under cross winds, so that the high-speed train in the complex wind environment will have adequate operating safety.

IV. CONCLUSION

(1) Under the effect of cross winds, the boundary layer flow and wake flow of train's surface are damaged, and large scale vortex appears in the leeward side of train. Along the train body backwards, and in different sections, the initial position of each vortex in the direction of the height shows alternative variation of the bottom, the middle and the top; the vortex in the area of bogie, pantograph and windshield is more complicated.

(2) The lift coefficient of the middle train is always larger than that of the head train, and it decreases as the train speed becomes higher. The lift of the tail train is smaller than that of the head train and middle train when the train speed is low. However, as the speed becomes higher, it surges rapidly. When the train speed is 350km/h, it even surpasses the lift of the head train and the middle train. The overturning moment coefficient of the head train crossing the longitudinal axis of the train center is the maximum, followed by that of the middle train, while that of the tail train is the minimum. Regarding to side-way moment, the head train is the maximum, followed by the tail train, while the middle train is the minimum. As for the pitching moment, the head train is the maximum.

(3) The higher the wind speed, the lower the maximum safe operating speed and on the opposite, the lower the wind speed, the higher the maximum safe operating speed; the maximum safe operating speed varies with different safety index limits. We suggest taking both derailment coefficient and the reduction rate of wheel load as the basis for determining the maximum safe operating speed under cross winds, so that the high-speed train in the complex wind environment will have adequate operating safety.

ACKNOWLEDGEMENT

The study was supported by the College students' innovative entrepreneurial training program.

Project supported by College Student Research and Career-creation program of Beijing City.

REFERENCES

- [1] A.P.Gaylard. The application of computational fluid dynamics to railway aerodynamics[J]. *Journal of rail and rapid transit, Proceedings of the Institution of Mechanical Engineers Part F*, 1993,57:103-121.
- [2] T.W.Chiu. Prediction of the aerodynamic loads on a railway train in a cross-wind at large yaw angles using an integrated two- and three-dimensional source-vortex panel method. *Journal of Wind Engineering and Industrial Aerodynamics*. 1995,57: 9-39
- [3] Baker C. J.. The simulation of unsteady aerodynamic cross wind forces on trains[J]. *Journal of Wind Engineering and Industrial Aerodynamics*, 2010, 98: 88-99.
- [4] W. Khier, M. Breuer, F.Durst. Flow structure around trains under side wind conditions: a numerical study[J]. *Computers and Fluids*,

2000,29:179-195.

- [5] Yu Zhou, Wei-qi Qian, You-qi Qian etc. Introductory analysis of the influence of Menter's k- ω SST turbulence model's parameters [J]. *Acta Aerodynamica Sinica*, 2010,28(2):213-217.